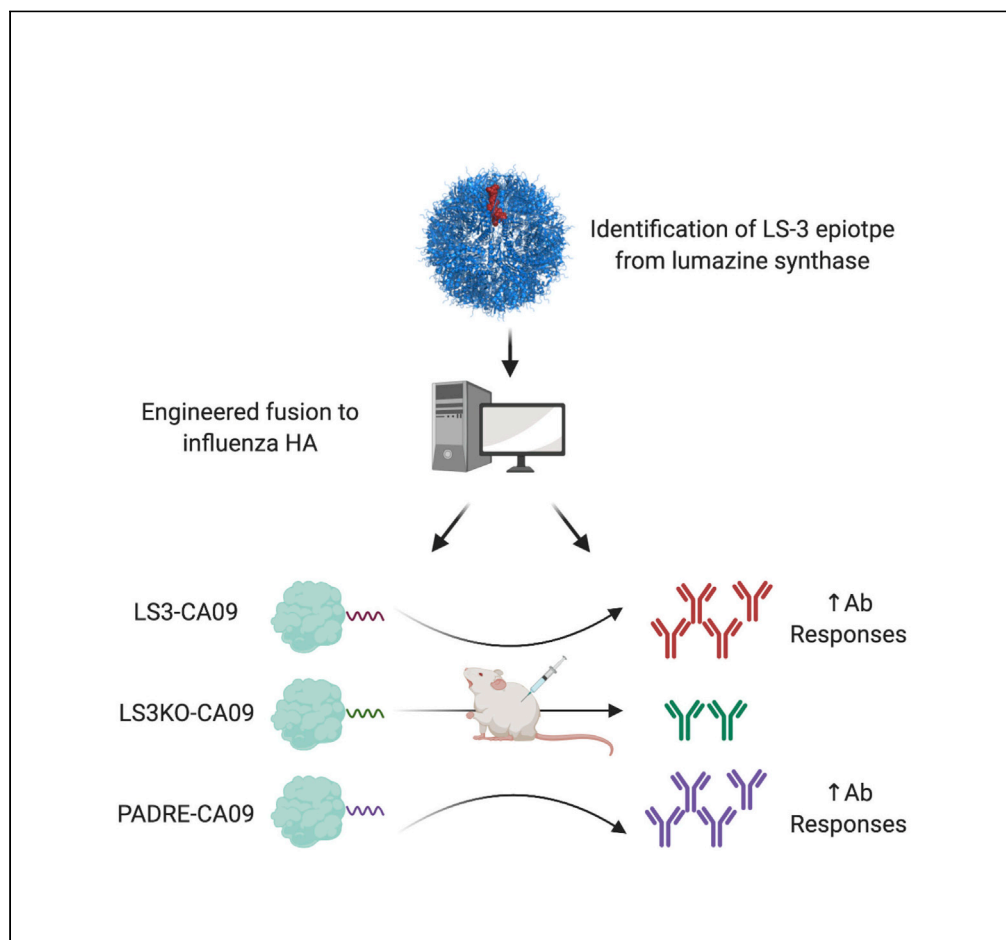


## Article

Incorporation of a Novel CD4+ Helper Epitope Identified from *Aquifex aeolicus* Enhances Humoral Responses Induced by DNA and Protein Vaccinations

Ziyang Xu, Neethu Chokkalingam, Edgar Tello-Ruiz, Susanne Walker, Daniel W. Kulp, David B. Weiner

dwkulp@wistar.org (D.W.K.)  
dweiner@wistar.org (D.B.W.)

**HIGHLIGHTS**

Identification of a novel CD4+ helper epitope, LS-3, from *Aquifex aeolicus*

*In silico* analysis predicts high binding affinity of LS-3 to human HLA-DR alleles

Fusing LS-3 to antigen enhances humoral response by vaccinations

Xu et al., iScience 23, 101399  
August 21, 2020 © 2020 The Authors.  
<https://doi.org/10.1016/j.isci.2020.101399>

## Article

Incorporation of a Novel CD4<sup>+</sup> Helper Epitope Identified from *Aquifex aeolicus* Enhances Humoral Responses Induced by DNA and Protein Vaccinations

Ziyang Xu,<sup>1,2,3</sup> Neethu Chokkalingam,<sup>1,3</sup> Edgar Tello-Ruiz,<sup>1</sup> Susanne Walker,<sup>1</sup> Daniel W. Kulp,<sup>1,\*</sup> and David B. Weiner<sup>1,4,\*</sup>

## SUMMARY

**CD4<sup>+</sup> T cells play an important role in the maturation of the antibody responses. Conjugation of identified CD4<sup>+</sup> T cell helper epitope to the target antigen has been developed as a strategy to enhance vaccine-induced humoral immunity. In this work, we reported the identification of a novel HLA-IAb helper epitope LS-3 from *Aquifex aeolicus*. *In silico* analysis predicted this epitope to have high binding affinity to common human HLA alleles and have complementary binding coverage to the established PADRE epitope. Introduction of HLA-IAb knockout mutations to the LS-3 epitope significantly attenuated humoral responses induced by a vaccine containing this epitope. Finally, engineered fusion of the epitope to a model antigen, influenza hemagglutinin, significantly improved both binding and hemagglutination inhibition antibody responses in mice receiving DNA or protein vaccines. In summary, LS-3 and additional identified CD4<sup>+</sup> helper epitopes may be further explored to improve vaccine responses in translational studies.**

## INTRODUCTION

Vaccination is an approach where antigenic materials are introduced into the hosts to elicit adaptive immune responses that may confer them with protection from subsequent pathogen exposure (Clem, 2011). Humoral immunity is an important branch of the adaptive immune system, in which antibodies produced by B cells serve either to directly neutralize targets on the pathogens through paratope-epitope interactions (Corti and Lanzavecchia, 2013; Kwong et al., 2013) or to indirectly mediate inactivation of the pathogens by engaging the complement system or effector cells such as macrophages and natural killer cells through Fc-dependent mechanisms (Kurdi et al., 2018; Seidel et al., 2013; van Erp et al., 2019). Antibody responses serve as an important correlate for protection for many emerging and re-emerging infectious diseases, including but not limited to HIV-1 (Burton and Hangartner, 2016), influenza (Laursen et al., 2018), and coronaviruses (Jiang et al., 2020). A strategy to enhance humoral responses induced by vaccination is, therefore, of great significance.

CD4<sup>+</sup> T cells, particularly T-follicular helper (T<sub>fh</sub>) cells, play a critical role in the maturation of antibody responses (Crotty, 2014). In the germinal center, immunological synapses are formed between T<sub>fh</sub> and Germinal Center B (GCB) cells through interactions of pairs of adhesion molecules such as LFA1-ICAM-1 and SAP-Ly108 to enable transfer of soluble cytokines, such as IL-4 and IL-21, from T<sub>fh</sub> to GCB cells and promote ligand-receptor interaction, such as CD40L-CD40 binding, to enhance survival, differentiation, somatic hypermutation, and class switching in the GCB cells (Carrasco et al., 2004; Elgueta et al., 2009; Flynn et al., 1998; Kageyama et al., 2012). Provision of T cell help, however, is contingent upon T<sub>fh</sub> activation by GCB cells through T cell receptor (TCR) peptide-MHC II interaction (Zhang et al., 2013). As such, robust germinal center B cell responses are dependent on presentation of MHC II-restricted epitope, derived from the antigen, by GCB to T<sub>fh</sub> cells. However, different epitopes have varying affinity for binding to MHC-II receptors depending on the hosts' haplotype such that peptide vaccines as well as smaller protein domains may not intrinsically contain a potent CD4<sup>+</sup> helper epitope to drive germinal center responses (Elbahnasawy et al., 2018; Falugi et al., 2001; Pichichero, 2013). Such is the rationale for conjugating peptide and carbohydrate vaccines to protein carriers, like Keyhole limpet hemocyanin (KLH) (Ragupathi et al., 2002), tetanus toxin (Diethelm-Okita et al., 2000), or hepatitis B-surface antigen (HbsAg) (Collins et al.,

<sup>1</sup>The Vaccine and Immunotherapy Center, Wistar Institute, Philadelphia, PA 19104, USA

<sup>2</sup>Department of Pharmacology, Perelman School of Medicine, University of Pennsylvania, Philadelphia, PA 19104, USA

<sup>3</sup>These authors contributed equally

<sup>4</sup>Lead Contact

\*Correspondence: dwkulp@wistar.org (D.W.K.), dweiner@wistar.org (D.B.W.)  
<https://doi.org/10.1016/j.isci.2020.101399>



2017). However, these large protein carriers may contain irrelevant immunodominant surfaces that may skew induced antibody responses away from the desired epitopes, creating additional uncertainties and challenges to this approach (Ghosh et al., 2013; Valea et al., 2018; Xu and Kulp, 2019).

Direct incorporation and fusion of a potent CD4<sup>+</sup> helper epitope with the target antigen may be a simpler and more effective strategy to enhance the induced humoral immunity. Several important epitopes have been identified in this manner. Incorporation of Pan DR epitope (PADRE), for example, has demonstrated to improve immunogenicity of peptide and protein vaccines in animal studies, and it has also been explored in several clinical studies (Alexander et al., 2000; Ghaffari-Nazari et al., 2015; Snook et al., 2019). Identification of additional potent CD4-helper epitopes can create new tools to be used in conjunction with, or as alternative to, these established CD4-helper epitopes to increase responses induced by various vaccine antigens.

In our prior work, we used synthetic DNA delivery by electroporation to mediate *in vivo* assembly of nanoparticle vaccines and observed that some nanoparticle scaffolding domains (used to promote self-assembly of scaffolded antigens) could induce CD4<sup>+</sup> T cell responses (Xu et al., 2020). In this work, we examined and performed epitope mapping on several bacterial or viral scaffold protein domains and determined that lumazine synthase (LS) from *Aquifex aeolicus* contained very potent CD4-helper epitopes for both BALB/c and C57BL/6 mice. LS can scaffold the assembly of 60 copies of HIV-priming antigen GT8, eOD-GT8-60mer, as well as other antigens (Jardine et al., 2016; Xu et al., 2020). *In silico* binding analysis determined that the identified C57BL/6 CD4-helper epitope (LS-3) was predicted also to have high binding affinity (<100 nM) to several common human MHC-II alleles (HLA-DRB1\*07:01, HLA-DRB1\*15:01, and HLA-DRB5\*01:01) and binds to a complementary set of HLA-DR alleles as compared with PADRE. We determined how this epitope might contribute to humoral immunity by engineering mutations that knocked out binding of this epitope to murine HLA I-Ab (LS3KO) and observed that DNA-launched GT8-60mer nanoparticles containing this mutant epitope (DLnano\_CD4MutLS\_GT8) induced weaker antibody responses than the corresponding DNA-launched wild-type GT8-60mer nanoparticles (DLnano\_LS\_GT8). Finally, engineered fusion of the identified LS-3 epitope to a different antigen, hemagglutinin (HA) receptor binding domain (RBD) from influenza H1/CA/07/09 (LS3-CA09), improved humoral responses induced to HA by DNA and protein vaccinations. Overall, this study provides a relatively rigorous demonstration that simple fusion of a dominant CD4-helper epitope to a target antigen could improve humoral responses induced by either protein or DNA vaccines in animal models and additionally describes the identification of a novel CD4-helper epitope from a bacterial enzyme, which may help inform the design of additional protein and DNA vaccines and be of translational importance.

## RESULTS

### Identification of Novel Murine CD4-Helper Epitopes from the LS Domain of *Aquifex aeolicus*

We previously observed that scaffold domains used to drive *in vivo* assembly of nanoparticle vaccines could sometimes induce CD4<sup>+</sup> T cell responses (Xu et al., 2020). Here, we compared CD4<sup>+</sup> T cell responses elicited by various nanoparticle scaffolding domains, ferritin from *Helicobacter pylori* (3BVE), LS from *Aquifex aeolicus*, and the viral cage of Prototype Foamy Virus (Pfv), in BALB/c immunized with DNA-launched GT8 nanoparticle vaccines that incorporate these respective protein domains (DLnano\_3BVE\_GT8, DLnano\_LS\_GT8, DLnano\_Pfv\_GT8) (Figure 1A). All mice in the experiments were immunized twice with 25 μg DNA immunogens 3 weeks apart and were euthanized 2 weeks post the second vaccination, at the time point that corresponded to their peak cellular responses. Using intracellular cytokine staining (ICS) to analyze murine splenocytes stimulated with overlapping peptide pools that spanned the respective protein domains, we determined that the LS domain elicited the most potent CD4<sup>+</sup> T cell responses (approximately 2% of CD3<sup>+</sup>CD4<sup>+</sup>CD62L<sup>-</sup>CD44<sup>+</sup> T cells were observed to IFNγ<sup>+</sup> following peptide stimulation), followed by the Pfv and the 3BVE domains. Importantly, DLnano\_LS\_GT8 vaccination elicited even more potent CD4<sup>+</sup> T cell responses to the LS domain in the C57BL/6 mice than in the BALB/c mice, as measured by expression of pro-inflammatory cytokines IFNγ, TNF-α, and IL-2 upon peptide stimulation (Figure 1B). LS-specific poly-functional CD4<sup>+</sup> T cell responses, as defined by the simultaneous expression of all three cytokines IFNγ, TNF-α, and IL-2, were induced in both the BALB/c and the C57BL/6 mice, accounting for approximately 1% and 3% of all CD3<sup>+</sup>CD4<sup>+</sup>CD62L<sup>-</sup>CD44<sup>+</sup> T cells, respectively (Figure 1C). We set out to identify the exact CD4-helper epitope in both the BALB/c and the C57BL/6 mice, using a combination of an IFNγ ELISpot assay for screening and a flow-based ICS assay for confirmation. Two predominant non-overlapping CD4<sup>+</sup> epitopes in the LS domain were observed for the BALB/c mice (LS-13:

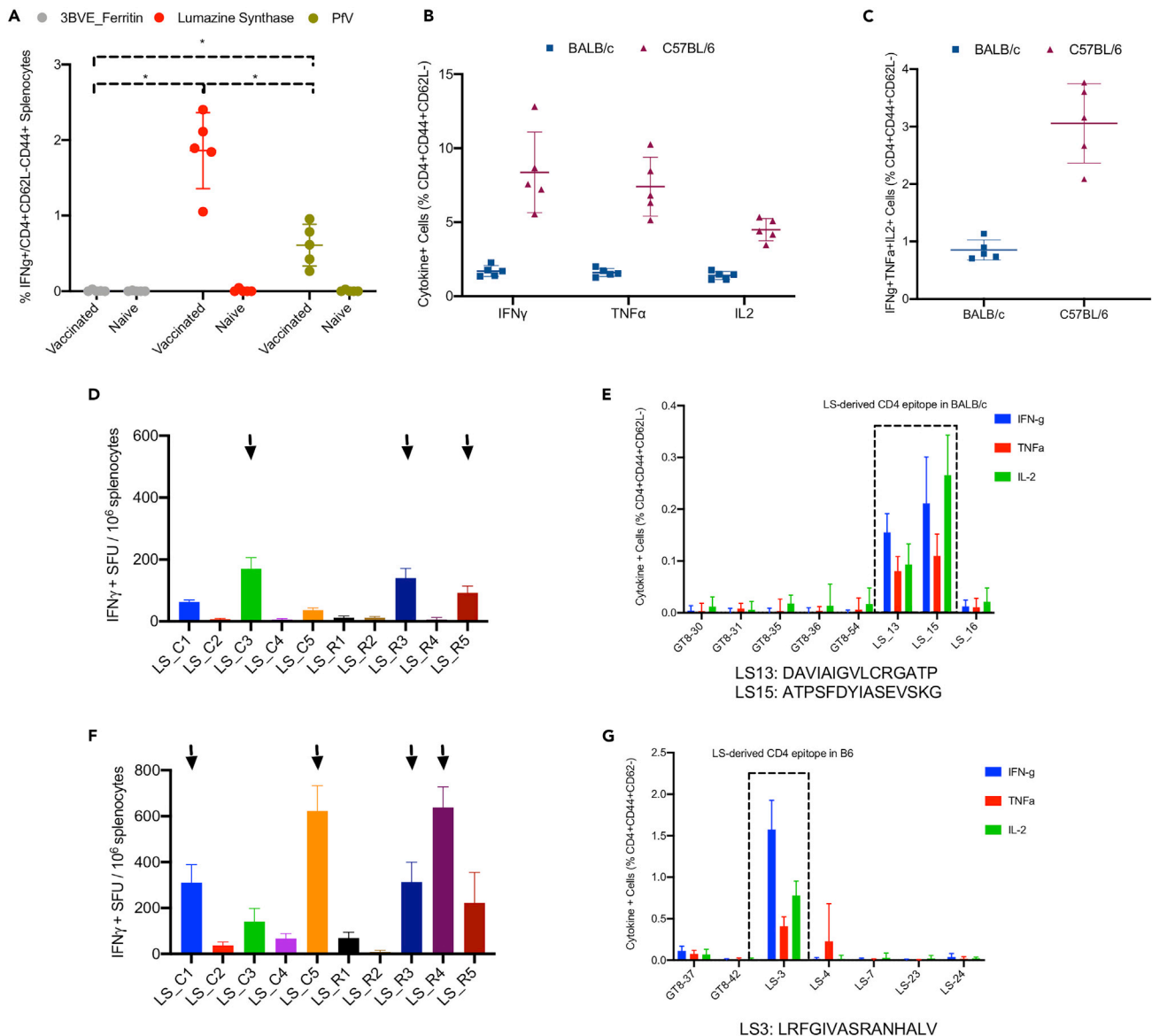


**Figure 1. Identification of LS-3 from Lumazine Synthase as a Potent CD4-Helper Epitope in C57BL/6 Mice**

Mice received 25  $\mu$ g DNA vaccination with EP twice 3 weeks apart and were euthanized 2 weeks post the second vaccination for cellular analysis.

(A) CD4<sup>+</sup> T cell IFN $\gamma$  responses induced to the 3BVE, LS, and PFV domains by DLnano\_3BVE\_GT8, DLnano\_LS\_GT8, and DLnano\_PFV\_GT8 vaccinations in BALB/c mice.

(B) Comparison of CD4<sup>+</sup> cytokine responses to the LS domain induced by DLnano\_LS\_GT8 in BALB/c versus C57BL/6 mice.

(C) Comparison of polyfunctional CD4<sup>+</sup> T cell responses to the LS domain induced by DLnano\_LS\_GT8 in BALB/c versus C57BL/6 mice.

(D and E) Matrix mapping by IFN $\gamma$  ELISpot assays (D) and ICS (E) to determine HLA I-Ad CD4<sup>+</sup> T cell epitopes in the LS domain in BALB/c mice immunized with DLnano\_LS\_GT8.

(F and G) Matrix mapping by IFN $\gamma$  ELISpot assays (F) and ICS (G) to determine HLA I-Ab CD4<sup>+</sup> T cell epitopes in the LS domain in C57BL/6 mice immunized with DLnano\_LS\_GT8. Each group includes five mice; each dot represents an animal; error bar represents standard deviation; two-tailed Mann-Whitney rank test used to compare groups; p values were adjusted for multiple comparison where appropriate; \*, p value < 0.05.

See also [Figure S1](#) and [Table S1](#).

DAVIAIGVLCRGATP and LS-15: ATPSFYDIASEVSKG) ([Figures 1D](#) and [1E](#)), whereas a single dominant CD4<sup>+</sup> epitope in the LS domain was observed for the C57BL/6 mice (LS-3: LRFGIVASRANHVALV) ([Figures 1F](#) and [1G](#)). The overall CD4<sup>+</sup> T cell responses measured by ICS were lower in the mapping study than in the previous experiment ([Figures 1B](#), [1E](#) and [1G](#)), likely because fresh splenocytes were used for ICS analysis previously ([Figure 1B](#)), whereas splenocytes were used 24 h post-harvest in the mapping experiment

**A**

		High affinity	Medium affinity	Low affinity
Peptide: LRFGIVASRANHALV				
	allele	smm_align_ic50 (nM)	nn_align_ic50 (nM)	
Humans	HLA-DRB1*03:01	360	504.7	
	HLA-DRB1*07:01	98	13.9	
	HLA-DRB1*15:01	114	63.6	
	HLA-DRB3*01:01	2310	4504.9	
	HLA-DRB4*01:01	559	504.4	
	HLA-DRB5*01:01	92	84.2	
Mice	H2-IAb	205	61.7	

**B**

Peptide: ATPSFDYIASEVSKG				
	allele	smm_align_ic50 (nM)	nn_align_ic50 (nM)	
Humans	HLA-DRB1*03:01	2831	4259.4	
	HLA-DRB1*07:01	143	309	
	HLA-DRB1*15:01	526	1916.5	
	HLA-DRB3*01:01	5060	2394.7	
	HLA-DRB4*01:01	1443	816.3	
	HLA-DRB5*01:01	158	1005.7	
Mice	H2-IAd	2001	7422.3	

Peptide: DAVIAIGVLCRGATP				
	allele	smm_align_ic50 (nM)	nn_align_ic50 (nM)	
Humans	HLA-DRB1*03:01	2330	871.1	
	HLA-DRB1*07:01	6134	5914.1	
	HLA-DRB1*15:01	1118	2411.7	
	HLA-DRB3*01:01	39360	18873	
	HLA-DRB4*01:01	2546	1978.4	
	HLA-DRB5*01:01	614	244.6	
Mice	H2-IAd	9029	1053.1	

**Figure 2. The LS-3 Epitope Was Observed to Have Potent Binding Affinities to Several Human HLA-DR Alleles with *In Silico* Analysis**

Predicted binding affinity, in terms of IC<sub>50</sub> value (nM), of the identified LS-3 (A), LS-13 and LS-15 (B) epitopes to common human and murine HLA alleles by NN- and SMM-align.

because of the time required for the preliminary IFN $\gamma$  ELISpot screen (Figures 1E and 1G). We also characterized additional epitopes identified through the preliminary IFN $\gamma$  ELISpot screen (Figures S1A and S1B) by ICS and mapped the CD8<sup>+</sup> T cell responses to two GT8 peptides in the BALB/c mice (Figure S1C and Table S1) and to one LS peptide in the C57BL/6 mice (Figure S1D and Table S1).

### Murine HLA-IAb Epitope Was Predicted to Have High Binding Affinity for Several Human MHC-II Alleles by *In Silico* Analysis

As the identified murine LS CD4-helper epitopes may or may not be conserved in humans, we used *in silico* analysis to predict the binding affinities of the identified LS-3, LS-13, and LS-15 epitopes to common human MHC-II alleles. Using a stabilization matrix method (SMM-align) and an artificial neural network-based method (NN-align) for alignment (Nielsen and Lund, 2009; Nielsen et al., 2007), the mapped murine C57BL/6 HLA-IAb epitope LS-3 demonstrated high binding affinity (<100 nM) for HLA-DRB1\*07:01, HLA-DRB1\*15:01, and HLA-DRB5\*01:01, which correspond to human allele frequencies of 6.98%, 7.86%, and 14.6% respectively (Louthrenoo et al., 2013; Solberg et al., 2008), and moderate binding affinity (<1,000 nM) for HLA-DRB1\*03:01 and HLA-DRB4\*01:01, which correspond to human allele frequencies of 6.76% and 35% respectively (Geng et al., 1995; Solberg et al., 2008). Low to moderate binding affinity (<5,000 nM) was observed for LS-3 to the human allele HLA-DRB3\*01:01 (Figure 2A). Of note, both the NN-align and the SMM-align correctly predicted high binding affinities of the LS-3 epitope to murine HLA-IAb. In contrast, the identified murine BALB/c HLA-IAd epitopes LS-13 and LS-15 were predicted to have lower binding affinities to either human or murine HLA alleles than the LS-3 epitope (Figure 2B). As such, since the LS-3 epitope was more likely to be conserved in humans, we decided to further characterize the HLA-IAb LS-3 epitope rather than the HLA-IAd LS-13/LS-15 epitopes in our downstream experiments.

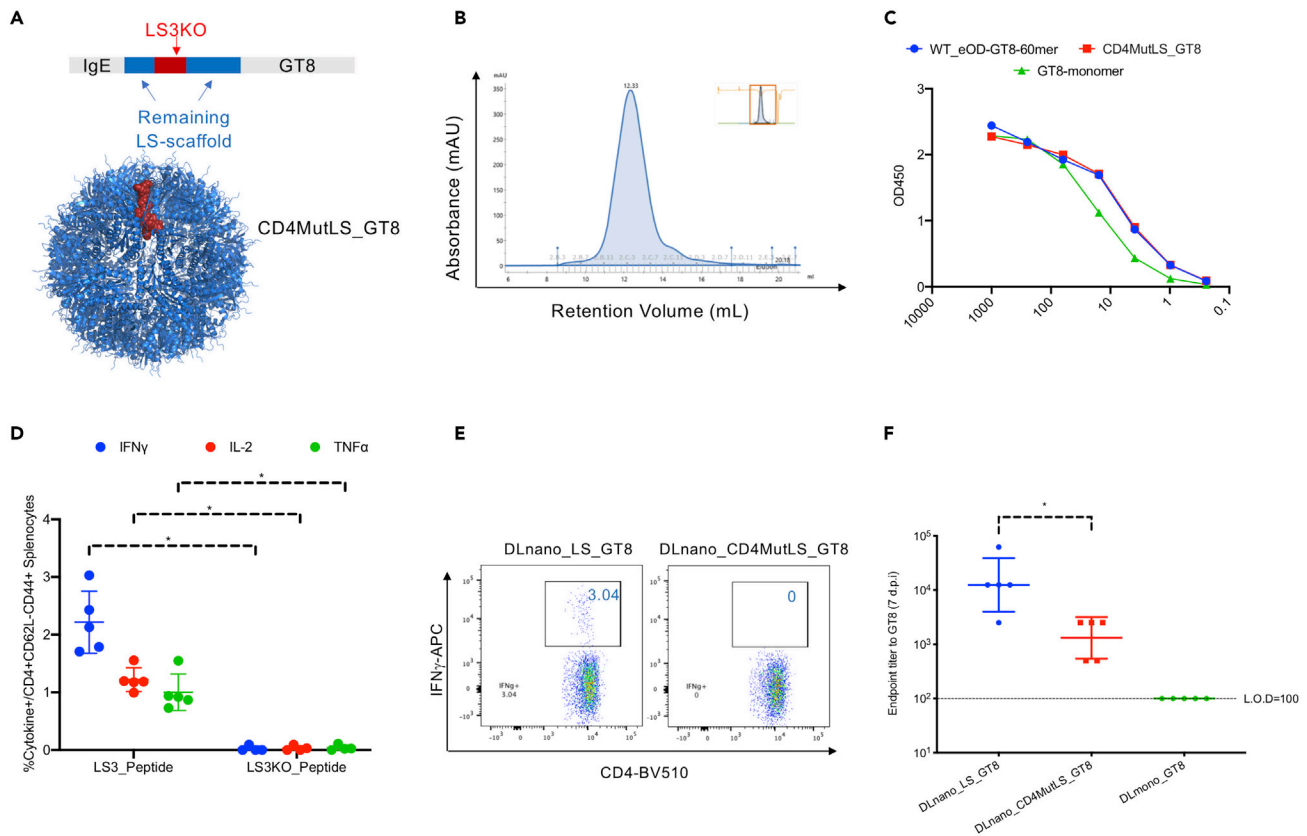


**Figure 3. Knockout of the LS-3 Epitope from DLnano\_LS\_GT8 was Observed to Attenuate Vaccine-Induced Humoral Immunity**

Mice received 25  $\mu$ g DNA vaccination with EP twice 3 weeks apart and were euthanized 2 weeks post the second vaccination for cellular analysis. (A) Engineering of CD4MutLS\_GT8 mutants by selected mutations of the LS-3 epitope (in red) that knocked out C57BL/6 HLA-IAb binding but still preserve assembly of the nanoparticle using structure-guided design, the remaining LS domain is shown in blue, the GT8 domain is not shown. (B) SEC-trace of lectin-column purified transfection supernatant of CD4MutLS\_GT8 to determine the assembly status of designed CD4MutLS\_GT8. (C) Characterization of binding of recombinantly produced CD4MutLS\_GT8, eOD-GT8-60mer, and GT8-mono to VRC01 by ELISA. (D and E) Cytokine expression by the ICS assay in C57BL/6 mice immunized with either DLnano\_LS\_GT8 or DLnano\_CD4MutLS\_GT8 to confirm knockout of the dominant LS-3 CD4<sup>+</sup> helper epitope in CD4MutLS\_GT8. (F) Humoral responses to GT8 for mice immunized with DLnano\_CD4MutLS\_GT8, DLnano\_LS\_GT8, or DLmono\_GT8 7 d.p.i. Each group includes five mice; each dot represents a mouse; error bar represents standard deviation; two-tailed Mann-Whitney rank test used to compare groups; p values were adjusted for multiple comparison where appropriate; \*, p value < 0.05. See also Figure S2.

### Identified Murine LS-3 CD4<sup>+</sup> Helper Epitope Supported the Induction of Potent Immune Responses by DLnano\_LS\_GT8

To determine whether CD4<sup>+</sup> T cell help provided by the identified LS-3 epitope can contribute to the induction of humoral immunity by DLnano\_LS\_GT8, we engineered a GT8 nanoparticle variant (DLnano\_CD4MutLS\_GT8) through a structure-guided design process in which the LS-3 epitope was selectively mutated to ablate its binding to HLA-IAb (as informed by the NN-align and the SMM-align-based binding analysis). Care was taken, simultaneously, to avoid mutations that may disrupt nanoparticle assembly. We mutated 27% residues in the LS-3 epitope (4/15 residues) and generated the corresponding knockout epitope LS3-KO (Figure 3A and Table S1), resulting in reduction of HLA-IAb binding affinity from 205 to 4,261 nM by the SMM-align and 61.7 to 7,668 nM by the NN-align. We verified the engineered variant DLnano\_CD4MutLS\_GT8 incorporating the LS3-KO epitope could still assemble homogeneously by expressing this new construct *in vitro* and performing size exclusion chromatography (SEC) of the lectin-column-purified DLnano\_CD4MutLS\_GT8 transfection supernatant. SEC showed CD4MutLS\_GT8 assembled homogeneously into 60-mer (single peak observed on the SEC trace centering at 12.33 mL retention volume) similar to what we previously observed for the wildtype eOD-GT8-60mer (Figure 3B) (Xu et al., 2020). Additionally, Size Exclusion Chromatography Multi Angle Light Scattering (SEC-MALS) analysis determined the

molecular weight of CD4MutLS\_GT8 to be around 2 MDa, close to the observed molecular weight of eOD-GT8-60mer (Figure S2A) (Xu et al., 2020). We examined the antigenic profiles of the engineered immunogens, and equivalent binding to VRC01, an HIV-1 broadly neutralizing antibody, was observed for eOD-GT8\_60mer and CD4MutLS\_GT8\_60mer (Figure 3C). ICS analyses of mice immunized with respective DNA-encoded constructs confirmed complete knockout of the LS-3 CD4+ helper epitope in the CD4MutLS\_GT8 construct (Figures 3D and 3E). Sera from animals seven d.p.i demonstrated significantly attenuated responses to GT8 in animals immunized with DLnano\_CD4MutLS\_GT8, although they still had stronger responses than those immunized with DNA-encoded GT8-monomer (Figure 3F). Differences in humoral immunity induced by DLnano\_LS\_GT8 and DLnano\_CD4MutLS\_GT8 waned overtime; however, repeat vaccination of DLnano\_LS\_GT8 but not DLnano\_CD4MutLS\_GT8 at 21 d.p.i boosted the humoral immunity in mice (Figure S2B). Taken together, this experiment suggests that the identified LS-3 CD4-helper epitope contributes to the overall antibody responses induced, as partial attenuation was observed when binding of this epitope to HLA IAb was knocked out.

### Engineered Fusion of LS-3 CD4+ Helper Epitope to CA09 HA-RBD Enhanced Anti-HA Antibody Responses Induced by DNA or Protein Vaccines

As we have determined that CD4+ T cell help provided by the LS-3 epitope could contribute to the overall humoral responses, we set out to determine if it can serve as an incorporated CD4-helper epitope to enhance induced antibody responses by engineering fusion of the epitope with a different model antigen, CA09 HA-RBD.

We first set out to compare LS-3 and PADRE epitopes in terms of their biophysical properties and predicted binding affinities to HLA-DR alleles by *in silico* analysis. LS-3 and PADRE epitopes are predicted to have similar biophysical properties, in that they both have low water solubility, contain several basic residues, and are expected to be slightly positively charged at pH 7.0 (Figure S3A). We used the PADRE epitope to help validate the accuracy of HLA-binding affinity prediction, by comparing *in silico* predicted IC50 values with experimentally measured values (Figure S3B) (Alexander et al., 1994). Experimentally measured IC50 values were observed to trend in a very similar fashion to *in silico* predicted values for the binding of PADRE to HLA-DRB1\*07:01, HLA-DRB5\*01:01, HLA-DRB3\*01:01, and murine H2-lab, particularly with the nn-align prediction algorithm. We next compared LS-3 and PADRE in terms of their binding affinities to various human HLA-DR alleles by computationally applying the MixMHCIpred model, which has been recently reported (Figure S3C) (Racle et al., 2019). The MixMHCIpred model incorporates features of smm- and nn-align and also uses a large dataset of empirically determined peptide-HLA-DR binding affinities to train a machine learning model, which was observed to have better performance, in terms of its receiver operating characteristic (ROC) curve in peptide HLA-DR binding prediction, than the classical NetMHCIIPan model. The LS-3 and PADRE epitopes were both predicted to have high binding affinities to several HLA-DR alleles, in terms of percentile rank (0–100, lower rank indicates stronger binding). Nevertheless, as compared with PADRE, LS-3 was observed to bind to several HLA-DR alleles more potently, particularly HLA-DRB1\*01:01, HLA-DRB1\*01:02, HLA-DRB1\*03:01, HLA-DRB1\*04:04, HLA-DRB1\*07:01, HLA-DRB3\*02:02, and HLA-DRB5\*02:02. In contrast, PADRE was observed to have higher binding affinity than LS-3 to other HLA-DR alleles, specifically HLA-DRB1\*04:01, HLA-DRB1\*04:08, and HLA-DRB1\*11:01. A negative control epitope, the first 15 residues of the human IgG1 Fc CH1 domain, was predicted to have low binding affinity (greater than 10% percentile rank) for all HLA-DR alleles, as expected.

We incorporated either an LS3KO epitope, an LS3 epitope, or a PADRE epitope (AKFVAAWTLKAAA) on the N terminus of CA09 HA-RBD, downstream of the IgE leader sequence, which served as a secretion tag for the antigen (Figure 4A). LS3KO-CA09 served as a better control to which responses induced by LS3-CA09 and PADRE-CA09 would be compared, as the impact of N-terminal peptide fusion on the immunogenicity of an antigen would be considered (protein sequences of LS3KO-CA09 and LS3-CA09 only differed at four residues). First, we confirmed that DNA-encoded LS3-CA09 could induce CD4+ T cell responses to the incorporated LS-3 epitope. Indeed, by ICS analysis, C57BL/6 mice immunized with DNA-encoded LS3-CA09 but not those immunized with LS3KO-CA09 were capable of mounting CD4+ T cell responses to their respective incorporated epitope (Figures 4B and 4C). The finding was similarly validated by IFN $\gamma$  ELIspot analysis (Figures S4A and S4B). Next, we compared CD4+ T cell responses induced by DNA-encoded LS3-CA09 and PADRE-CA09 to the LS3 and PADRE epitopes, respectively. Both LS-3 and PADRE elicited potent CD4+ T cell responses upon vaccination of DNA-encoded LS3-CA09 and PADRE-CA09 in C57BL/6 mice, with similar levels of cytokine responses induced as determined by ICS (Figures 4D

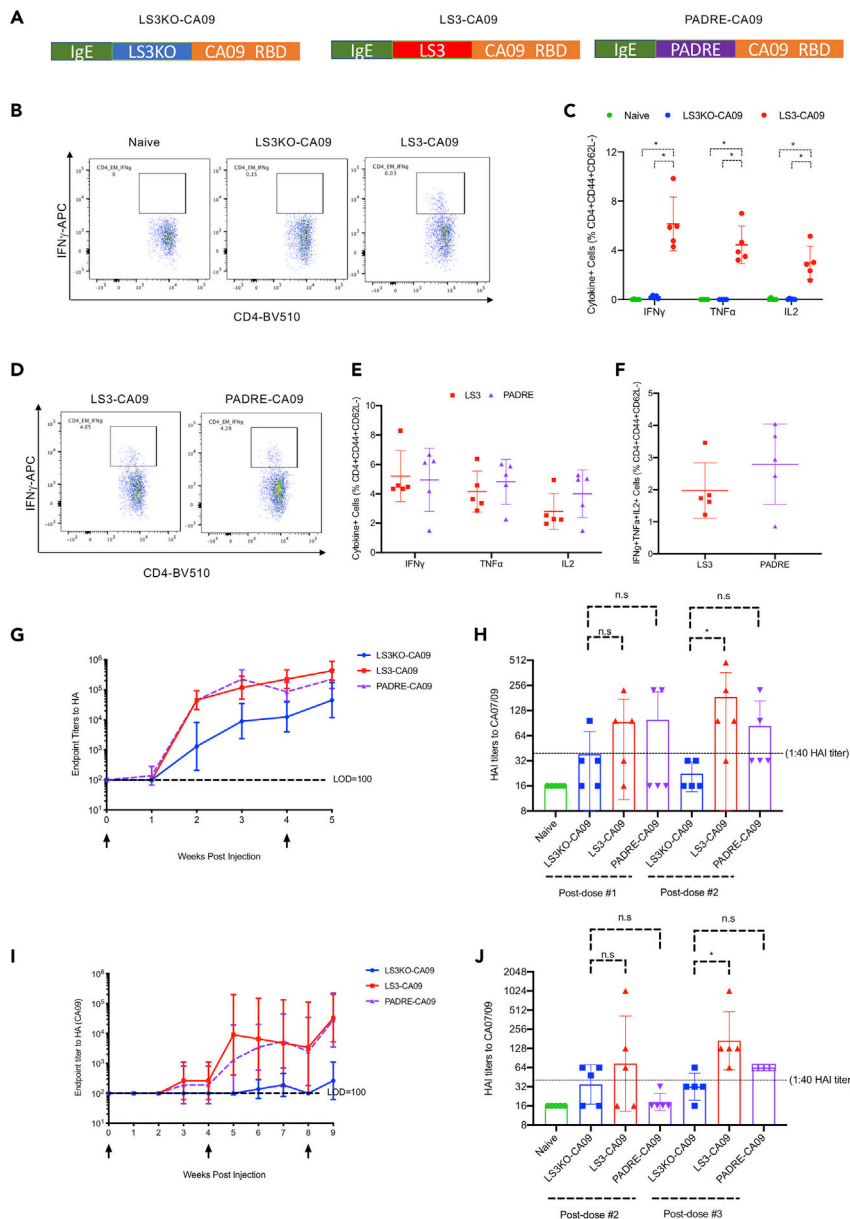


**Figure 4. Incorporation of either PADRE or LS-3 Epitopes to a Model CA09 Influenza HA Immunogen (HA-RBD) Induced Epitope-Specific CD4+ T cell Responses and Improved Antigen-Specific Binding and HAI Antibody Responses**

C57BL/6 mice received either 25  $\mu$ g DNA vaccination with EP twice 4 weeks apart and were euthanized 1 week post the second vaccination or 10  $\mu$ g RIBI-adjuvanted protein vaccinations three times 4 weeks apart and were euthanized 1 week post the third vaccination.

(A) Layouts of the engineered LS3-CA09, LS3KO-CA09, and PADRE-CA09 fusion constructs.

(B and C) Flow plots (B) and groups statistics (C) to compare CD4+ T cell cytokine responses induced by either DNA-encoded LS3-CA09 or LS3KO-CA09 immunizations in mice to LS3 and LS3KO peptides, respectively.

(D and E) Flow plots (D) and groups statistics (E) to compare CD4+ T cell cytokine responses induced by either DNA-encoded LS3-CA09 or PADRE-CA09 immunizations in mice to LS3 and PADRE peptides, respectively.

(F) Comparison of poly-functional IFN $\gamma$ +TNF $\alpha$ +IL-2+ CD4+ T cell responses to either LS3 or PADRE peptides in mice immunized as described in (D) and (E).

(G and H) Comparison of anti-HA binding antibody responses (G) and HAI titers (H) in mice immunized with DNA-encoded LS3KO-CA09, LS3-CA09, or PADRE CA09.

**Figure 4. Continued**

(I and J) Comparison of anti-HA binding antibody responses (I) and HAI titers (J) in mice immunized with RIBI-adjuvanted protein LS3KO-CA09, LS3-CA09, or PADRE CA09. Each group includes five mice; each dot represents a mouse; error bar represents standard deviation; two-tailed Mann-Whitney rank test used to compare groups; p values were adjusted for multiple comparison where appropriate; \*, p value<0.05.

See also [Figures S3 and S4](#).

and 4E) and IFN $\gamma$  ELIspot assays ([Figure S4c and S4d](#)). Additionally, by ICS analysis, epitope-specific poly-functional T cell responses were also similar between the LS-3 and PADRE epitopes ([Figure 4F](#)).

Next, we compared the humoral responses induced by two vaccinations of DNA-encoded LS3KO-CA09, LS3-CA09, and PADRE-CA09 to CA09 HA over time. By ELISA analysis, both DNA-encoded LS3-CA09 and PADRE-CA09 improved induced binding antibody responses to HA as compared with DNA-encoded LS3KO-CA09 prior to and after the boost, with approximately 9.5-fold and 5-fold improvements observed for DNA-encoded LS3-CA09 and PADRE-CA09, respectively ([Figure 4G](#)). Most importantly, we observed that functional antibody responses, as measured by the hemagglutination inhibition (HAI) titers, were significantly improved for DNA-encoded LS3-CA09 relative to LS3KO-CA09 after the second vaccination (with a mean titer of 126 versus 21, respectively) ([Figure 4H](#)). DNA-encoded PADRE-CA09, on the other hand, did not significantly improve the HAI titers relative to DNA-encoded LS3KO-CA09 after the first or the second vaccination ([Figure 4H](#)).

We further determined whether the observed phenomenon can be generalized to other routes of vaccination, such as protein vaccines. C-terminal his-tagged LS3KO-CA09, LS3-CA09, and PADRE-CA09 were expressed *in vitro* and purified from Expi293F cell transfection supernatant with nickel column. C57BL/6 mice were subsequently immunized with 10  $\mu$ g recombinant protein LS3KO-CA09, LS3-CA09, or PADRE-CA09 co-formulated with RIBI each time. RIBI adjuvant, or Sigma Adjuvant System, is a stable water-in-oil emulsion with significantly lower local reactogenicity and can be used as an alternative to classical Freund's adjuvant ([Lipman et al., 1992](#)); it has also been demonstrated to induce higher IgG titers and a Th1-biased immune response in comparison with incomplete Freund's adjuvant ([Chaitra et al., 2007](#)), the latter of which has been used in several clinical trials ([Apostolico Jde et al., 2016](#); [Rosenberg et al., 2010](#)). Humoral and cellular responses induced by protein vaccination were observed to be considerably lower than those induced by DNA vaccinations ([Figures 4G and 4I](#)), such that three protein vaccinations at weeks 0, 4, and 8 were required for us to observe robust humoral responses. Epitope-specific CD4<sup>+</sup> T cell responses induced by protein vaccinations were considerably lower than that by DNA vaccines. However, CD4<sup>+</sup> T cell responses directed at the LS-3 epitope could still be observed by ICS ([Figure S4E](#)) and by IFN $\gamma$  ELIspot ([Figure S4F and S4G](#)). CD4<sup>+</sup> T cell responses to PADRE were not observed ([Figures S4E–S4G](#)), likely as a result of the sensitivity of detection of the assays. Regardless, it was observed that HA-binding antibody titers induced by both protein LS3-CA09 and PADRE-CA09 vaccinations were significantly higher (100% sero-conversion in both groups) relative to protein LS3KO-CA09 vaccination, for which 20% sero-conversion (1/5 mice) was observed ([Figure 4I](#)). Lastly, similar to what was observed for DNA vaccinations, protein LS3-CA09 vaccination induced significantly improved HAI titers post-dose 3 relative to protein LS3KO-CA09 vaccination (with a mean titer of 169 versus 32, respectively). Protein PADRE-CA09 vaccination, on the other hand, was not observed to induce significantly improved HAI titers ([Figure 4J](#)). Taken together, the data suggest that the engineered fusion of the identified LS-3 CD4<sup>+</sup> helper epitope to a model antigen can significantly enhance humoral responses to that antigen. Additionally, the incorporation of the LS-3 epitope performed as well as, if not better than, the incorporation of the PADRE epitope in terms of adjuvating humoral responses.

## DISCUSSION

The importance of CD4<sup>+</sup> T cell help in facilitating antibody maturation and class switching is well established ([Crum-Cianflone and Wallace, 2014](#)). Patients with AIDS with low CD4<sup>+</sup> T cell count cannot mount effective antibody responses with vaccination. Similarly, laboratory animals that receive transient CD4<sup>+</sup> T cell depletion also cannot develop strong antibody responses to a foreign gene or an antigen ([Duperrret et al., 2018](#); [Wise et al., 2020](#); [Xu et al., 2018](#)). Both secreted soluble cytokine factors as well as surface-displayed ligands from Tfh cells are indispensable to the survival, AID-dependent somatic hypermutation, and proliferation of GCB cells and are necessary for the generation of antibody-secreting plasma cells and long-lived memory B cells ([Crotty, 2015](#)).

Although larger antigenic protein domains likely harbor CD4<sup>+</sup> T cell epitopes that can be restricted by the host HLA alleles for the induction of Tfh responses, carbohydrate and peptide vaccines are intrinsically

minimalistic and unlikely to contain potent CD4+ T cell help epitopes (Astronomo and Burton, 2010). Additionally, domain minimization has now become an increasingly important approach in protein engineering and vaccinology, as researchers begin to appreciate the importance of focusing elicited B cell responses to certain target epitopes by designing protein mini-domain devoid of distracting immunodominant surfaces (van der Lubbe et al., 2018; Yassine et al., 2015). However, these mini-proteins contain fewer overlapping peptides and therefore statistically will be less likely to harbor potent HLA-restricted CD4+ helper epitopes. As such, several studies have explored conjugation of these carbohydrate, peptide, or mini-protein vaccines to carrier proteins, including but not limited to KLH, tetanus toxin, and HbsAg. Induction of more potent antibody responses was observed in many cases (Jin et al., 2017; Marini et al., 2019). However, this approach may undermine the core motivations behind domain minimization by introducing a host of immunodominant distracting surfaces that may skew induced humoral responses.

Conjugation of the antigen with a shorter conserved CD4+ T cell epitope may offer a promising alternative to conjugation with a whole protein carrier. As the CD4+ T cell epitope is intrinsically shorter (12–16 amino acid long), it will less represent a distracting immunodominant surface (Hemmer et al., 2000). Additionally, they may alternatively be used as short linker to connect different protein domains, such as to cross-link a nanoparticle protein scaffold with a target antigen to promote vaccine antigen self-assembly (He et al., 2018). Fusing antigen with the PADRE epitope has been demonstrated to improve antibody responses in several animal studies and has also been explored in the clinic (clinical trials NCT01972737 and NCT02264236) (Rosa et al., 2004). Additional CD4+ helper epitopes have also been mapped and explored. For example, a recent study reported that co-delivery of MPER antigen with a *Leishmania major*-derived HLA I-Ad helper CD4+ T cell epitope (LACK) in liposomes can improve induced anti-MPER antibody responses (Elbahnasawy et al., 2018).

In this study, we reported the identification and characterization of a novel HLA I-Ab epitope LS-3 from the LS domain of *Aquifex aeolicus*, which is also the protein domain that can be used to scaffold the assembly of a 60-mer nanoparticle. *In silico* analysis predicted the LS-3 epitope to have high binding affinity to several common human HLA alleles. Epitope knockout experiment demonstrated that CD4+ T cell help provided by this epitope could indeed contribute to the overall antibody responses. Additionally, with *in silico* analysis, the LS-3 and PADRE epitopes were predicted to bind to a complementary set of HLA-DR alleles, such that it may be envisioned for them to be used in conjunction to further increase breadth of HLA-DR coverage in diverse human populations. Finally, engineered genetic fusion of the LS-3 epitope with a different target antigen CA09 HA-RBD (LS3-CA09) significantly increased binding and HAI antibody titers elicited by protein and DNA vaccinations to HA as compared with the control antigen, LS3KO-CA09. The study demonstrates the potential utility in this epitope to increase vaccine-induced antibody responses, in both preclinical murine studies as well as possibly in translational vaccine trials.

### Limitations of the Study

The main limitation in this study is that the binding affinity of the LS-3 epitope to human HLA alleles was predicted through *in silico* analysis, the accuracy of which was determined to be around 65% in one report (Andreatta et al., 2015), since the empirical *in vitro* human HLA binding assays were cost prohibitive. It should be noted, however, even with *in vitro* binding analysis, a human vaccine trial would be required to validate whether an identified epitope can indeed elicit CD4+ T cell responses in humans. Notably, the LS-domain scaffolded protein eOD-GT8-60mer is currently undergoing a phase I clinical study (NCT03547245), and additional insights may be obtained in the near future as to whether the LS domain, and particularly the LS-3 epitope, can elicit CD4+ T cell responses in the human population with varying HLA-allele distribution and be used to increase vaccine-induced humoral responses more broadly as described in this paper.

### Resource Availability

#### Lead Contact

Further information and requests for resources and reagents should be directed to and will be fulfilled by the Lead Contact, David B. Weiner, Email: [dweiner@wistar.org](mailto:dweiner@wistar.org). Address: 3601 Spruce St, Room 630, Philadelphia, PA 19104.

#### Materials Availability

All unique reagents generated in this study are available from the Lead Contact with a completed Materials Transfer Agreement.

### Data and Code Availability

No new code, software, algorithm, and large dataset were generated in this research.

### METHODS

All methods can be found in the accompanying [Transparent Methods supplemental file](#).

### SUPPLEMENTAL INFORMATION

Supplemental Information can be found online at <https://doi.org/10.1016/j.isci.2020.101399>.

### ACKNOWLEDGMENTS

This research is supported by NIH IPCAVD Grant U19 AI109646-04, NIH/NIAID Collaborative Influenza Vaccine Innovation Centers (CIVIC) contract 75N93019C00051, and Inovio Pharmaceuticals Vaccine Grant 5182101374 awarded to D.B.W, W. W. Smith Charitable Trust 68112-01-383 awarded to D.W.K, and by Wistar Monica H.M. Shander Memorial Fellowship awarded to Z.X.

### AUTHOR CONTRIBUTIONS

Z.X., D.B.W., and D.W.K. conceptualized the project. Z.X., D.B.W., and D.W.K. planned the experiments. Z.X., N.C., E.T.-R., and S.W. conducted the experiments. Z.X. analyzed the data. Z.X., N.C., D.B.W., and D.W.K. wrote the paper.

### DECLARATION OF INTERESTS

Z.X., D.W.K., and D.B.W. have a pending US patent on genetic fusion constructs with the identified LS-3 epitope. D.B.W. has received grant funding, participates in industry collaborations, has received speaking honoraria, and has received fees for consulting, including serving on scientific review committees and board series. Remuneration received by D.B.W. includes direct payments, stock or stock options, and in the interest of disclosure he notes potential conflicts associated with his work with Inovio and possible others.

Received: May 13, 2020

Revised: June 25, 2020

Accepted: July 20, 2020

Published: August 21, 2020

### REFERENCES

- Alexander, J., del Guercio, M.F., Maewal, A., Qiao, L., Fikes, J., Chesnut, R.W., Paulson, J., Bundle, D.R., DeFrees, S., and Sette, A. (2000). Linear PADRE T helper epitope and carbohydrate B cell epitope conjugates induce specific high titer IgG antibody responses. *J. Immunol.* *164*, 1625–1633.
- Alexander, J., Sidney, J., Southwood, S., Ruppert, J., Oseroff, C., Maewal, A., Snoko, K., Serra, H.M., Kubo, R.T., Sette, A., et al. (1994). Development of high potency universal DR-restricted helper epitopes by modification of high affinity DR-blocking peptides. *Immunity* *1*, 751–761.
- Andreatta, M., Karosiene, E., Rasmussen, M., Stryhn, A., Buus, S., and Nielsen, M. (2015). Accurate pan-specific prediction of peptide-MHC class II binding affinity with improved binding core identification. *Immunogenetics* *67*, 641–650.
- Apostolico Jde, S., Lunardelli, V.A., Coirada, F.C., Boscardin, S.B., and Rosa, D.S. (2016). Adjuvants: classification, modus operandi, and licensing. *J. Immunol. Res.* *2016*, 1459394.
- Astronomo, R.D., and Burton, D.R. (2010). Carbohydrate vaccines: developing sweet solutions to sticky situations? *Nat. Rev. Drug Discov.* *9*, 308–324.
- Burton, D.R., and Hangartner, L. (2016). Broadly neutralizing antibodies to HIV and their role in vaccine design. *Annu. Rev. Immunol.* *34*, 635–659.
- Carrasco, Y.R., Fleire, S.J., Cameron, T., Dustin, M.L., and Batista, F.D. (2004). LFA-1/ICAM-1 interaction lowers the threshold of B cell activation by facilitating B cell adhesion and synapse formation. *Immunity* *20*, 589–599.
- Chaitra, M.G., Nayak, R., and Shaila, M.S. (2007). Modulation of immune responses in mice to recombinant antigens from PE and PPE families of proteins of *Mycobacterium tuberculosis* by the Ribi adjuvant. *Vaccine* *25*, 7168–7176.
- Clem, A.S. (2011). Fundamentals of vaccine immunology. *J. Glob. Infect. Dis.* *3*, 73–78.
- Collins, K.A., Snaith, R., Cottingham, M.G., Gilbert, S.C., and Hill, A.V.S. (2017). Enhancing protective immunity to malaria with a highly immunogenic virus-like particle vaccine. *Sci. Rep.* *7*, 46621.
- Corti, D., and Lanzavecchia, A. (2013). Broadly neutralizing antiviral antibodies. *Annu. Rev. Immunol.* *31*, 705–742.
- Crotty, S. (2014). T follicular helper cell differentiation, function, and roles in disease. *Immunity* *41*, 529–542.
- Crotty, S. (2015). A brief history of T cell help to B cells. *Nat. Rev. Immunol.* *15*, 185–189.
- Crum-Cianflone, N.F., and Wallace, M.R. (2014). Vaccination in HIV-infected adults. *AIDS Patient Care STDS* *28*, 397–410.
- Diethelm-Okita, B.M., Okita, D.K., Banaszak, L., and Conti-Fine, B.M. (2000). Universal epitopes for human CD4+ cells on tetanus and diphtheria toxins. *J. Infect. Dis.* *181*, 1001–1009.
- Duperret, E.K., Trautz, A., Stoltz, R., Patel, A., Wise, M.C., Perales-Puchalt, A., Smith, T., Broderick, K.E., Masteller, E., Kim, J.J., et al. (2018). Synthetic DNA-encoded monoclonal antibody delivery of anti-CTLA-4 antibodies induces tumor shrinkage in vivo. *Cancer Res.* *78*, 6363–6370.

- Elbahnasawy, M.A., Donius, L.R., Reinherz, E.L., and Kim, M. (2018). Co-delivery of a CD4 T cell helper epitope via covalent liposome attachment with a surface-arrayed B cell target antigen fosters higher affinity antibody responses. *Vaccine* 36, 6191–6201.
- Elgueta, R., Benson, M.J., de Vries, V.C., Wasiuk, A., Guo, Y., and Noelle, R.J. (2009). Molecular mechanism and function of CD40/CD40L engagement in the immune system. *Immunol. Rev.* 229, 152–172.
- Falugi, F., Petracca, R., Mariani, M., Luzzi, E., Mancianti, S., Carinci, V., Melli, M.L., Finco, O., Wack, A., Di Tommaso, A., et al. (2001). Rationally designed strings of promiscuous CD4(+) T cell epitopes provide help to *Haemophilus influenzae* type b oligosaccharide: a model for new conjugate vaccines. *Eur. J. Immunol.* 31, 3816–3824.
- Flynn, S., Toellner, K.M., Raykundalia, C., Goodall, M., and Lane, P. (1998). CD4 T cell cytokine differentiation: the B cell activation molecule, OX40 ligand, instructs CD4 T cells to express interleukin 4 and upregulates expression of the chemokine receptor, Blr-1. *J. Exp. Med.* 188, 297–304.
- Geng, L., Imanishi, T., Tokunaga, K., Zhu, D., Mizuki, N., Xu, S., Geng, Z., Gojobori, T., Tsuji, K., and Inoko, H. (1995). Determination of HLA class II alleles by genotyping in a Manchu population in the northern part of China and its relationship with Han and Japanese populations. *Tissue Antigens* 46, 111–116.
- Ghaffari-Nazari, H., Tavakkol-Afshari, J., Jaafari, M.R., Tahaghoghi-Hajghorbani, S., Masoumi, E., and Jalali, S.A. (2015). Improving multi-epitope long peptide vaccine potency by using a strategy that enhances CD4+ T help in BALB/c mice. *PLoS One* 10, e0142563.
- Ghosh, M., Solanki, A.K., Roy, K., Dhoke, R.R., Ashish, and Roy, S. (2013). Carrier protein influences immunodominance of a known epitope: implication in peptide vaccine design. *Vaccine* 31, 4682–4688.
- He, L., Kumar, S., Allen, J.D., Huang, D., Lin, X., Mann, C.J., Saye-Francisco, K.L., Copps, J., Sarkar, A., Blizard, G.S., et al. (2018). HIV-1 vaccine design through minimizing envelope metastability. *Sci. Adv.* 4, eaau6769.
- Hemmer, B., Kondo, T., Gran, B., Pinilla, C., Cortese, I., Pascal, J., Tzou, A., McFarland, H.F., Houghten, R., and Martin, R. (2000). Minimal peptide length requirements for CD4(+) T cell clones—implications for molecular mimicry and T cell survival. *Int. Immunol.* 12, 375–383.
- Jardine, J.G., Kulp, D.W., Havenar-Daughton, C., Sarkar, A., Briney, B., Sok, D., Sesterhenn, F., Ereno-Orbea, J., Kalyuzhnyi, O., Deresa, I., et al. (2016). HIV-1 broadly neutralizing antibody precursor B cells revealed by germline-targeting immunogen. *Science* 351, 1458–1463.
- Jiang, S., Hillyer, C., and Du, L. (2020). Neutralizing antibodies against SARS-CoV-2 and other human coronaviruses. *Trends Immunol.* 41, 355–359.
- Jin, C., Gibani, M.M., Moore, M., Juel, H.B., Jones, E., Meiring, J., Harris, V., Gardner, J., Nebykova, A., Kerridge, S.A., et al. (2017). Efficacy and immunogenicity of a Vi-tetanus toxoid conjugate vaccine in the prevention of typhoid fever using a controlled human infection model of *Salmonella Typhi*: a randomised controlled, phase 2b trial. *Lancet* 390, 2472–2480.
- Kageyama, R., Cannons, J.L., Zhao, F., Yusuf, I., Lao, C., Locci, M., Schwartzberg, P.L., and Crotty, S. (2012). The receptor Ly108 functions as a SAP adaptor-dependent on-off switch for T cell help to B cells and NKT cell development. *Immunity* 36, 986–1002.
- Kurdi, A.T., Glavey, S.V., Bezman, N.A., Jhatakia, A., Guerriero, J.L., Manier, S., Moschetta, M., Mishima, Y., Roccaro, A., Detappe, A., et al. (2018). Antibody-dependent cellular Phagocytosis by macrophages is a novel mechanism of action of elotuzumab. *Mol. Cancer Ther.* 17, 1454–1463.
- Kwong, P.D., Mascola, J.R., and Nabel, G.J. (2013). Broadly neutralizing antibodies and the search for an HIV-1 vaccine: the end of the beginning. *Nat. Rev. Immunol.* 13, 693–701.
- Laursen, N.S., Friesen, R.H.E., Zhu, X., Jongeneelen, M., Blokland, S., Vermond, J., van Eijgen, A., Tang, C., van Diepen, H., Obmolova, G., et al. (2018). Universal protection against influenza infection by a multidomain antibody to influenza hemagglutinin. *Science* 362, 598–602.
- Lipman, N.S., Trudel, L.J., Murphy, J.C., and Sahali, Y. (1992). Comparison of immune response potentiation and in vivo inflammatory effects of Freund's and RIBI adjuvants in mice. *Lab. Anim. Sci.* 42, 193–197.
- Louthrenoo, W., Kasitanon, N., Wichainun, R., Wangkaew, S., Sukitawat, W., Ohnogi, Y., Hong, G.H., Kuwata, S., and Takeuchi, F. (2013). The genetic contribution of HLA-DRB5\*01:01 to systemic lupus erythematosus in Thailand. *Int. J. Immunogenet.* 40, 126–130.
- Marini, A., Zhou, Y., Li, Y., Taylor, I.J., Leneghan, D.B., Jin, J., Zanic, M., Mekhaie, D., Long, C.A., Miura, K., et al. (2019). A universal plug-and-display vaccine carrier based on HBsAg VLP to maximize effective antibody response. *Front. Immunol.* 10, 2931.
- Nielsen, M., and Lund, O. (2009). NN-align. An artificial neural network-based alignment algorithm for MHC class II peptide binding prediction. *BMC Bioinformatics* 10, 296.
- Nielsen, M., Lundegaard, C., and Lund, O. (2007). Prediction of MHC class II binding affinity using SMM-align, a novel stabilization matrix alignment method. *BMC Bioinformatics* 8, 238.
- Pichichero, M.E. (2013). Protein carriers of conjugate vaccines: characteristics, development, and clinical trials. *Hum. Vaccin. Immunother.* 9, 2505–2523.
- Racle, J., Michaux, J., Rockinger, G.A., Arnaud, M., Bobisse, S., Chong, C., Guillaume, P., Coukos, G., Harari, A., Jandus, C., et al. (2019). Robust prediction of HLA class II epitopes by deep motif deconvolution of immunopeptidomes. *Nat. Biotechnol.* 37, 1283–1286.
- Ragupathi, G., Cappello, S., Yi, S.S., Canter, D., Spassova, M., Bornmann, W.G., Danishefsky, S.J., and Livingston, P.O. (2002). Comparison of antibody titers after immunization with monovalent or tetravalent KLH conjugate vaccines. *Vaccine* 20, 1030–1038.
- Rosa, D.S., Tzelepis, F., Cunha, M.G., Soares, I.S., and Rodrigues, M.M. (2004). The pan HLA DR-binding epitope improves adjuvant-assisted immunization with a recombinant protein containing a malaria vaccine candidate. *Immunol. Lett.* 92, 259–268.
- Rosenberg, S.A., Yang, J.C., Kammula, U.S., Hughes, M.S., Restifo, N.P., Schwarz, S.L., Morton, K.E., Laurencot, C.M., and Sherry, R.M. (2010). Different adjuvanticity of incomplete freund's adjuvant derived from beef or vegetable components in melanoma patients immunized with a peptide vaccine. *J. Immunother.* 33, 626–629.
- Seidel, U.J., Schlegel, P., and Lang, P. (2013). Natural killer cell mediated antibody-dependent cellular cytotoxicity in tumor immunotherapy with therapeutic antibodies. *Front. Immunol.* 4, 76.
- Snook, A.E., Baybutt, T.R., Xiang, B., Abraham, T.S., Flickinger, J.C., Jr., Hyslop, T., Zhan, T., Kraft, W.K., Sato, T., and Waldman, S.A. (2019). Split tolerance permits safe Ad5-GUCY2C-PADRE vaccine-induced T-cell responses in colon cancer patients. *J. Immunother. Cancer* 7, 104.
- Solberg, O.D., Mack, S.J., Lancaster, A.K., Single, R.M., Tsai, Y., Sanchez-Mazas, A., and Thomson, G. (2008). Balancing selection and heterogeneity across the classical human leukocyte antigen loci: a meta-analytic review of 497 population studies. *Hum. Immunol.* 69, 443–464.
- Valea, I., Adjei, S., Usuf, E., Traore, O., Ansong, D., Tinto, H., Owusu Boateng, H., Leach, A., Mwinnessobaonfou Some, A., Buabeng, P., et al. (2018). Immune response to the hepatitis B antigen in the RTS,S/AS01 malaria vaccine, and co-administration with pneumococcal conjugate and rotavirus vaccines in African children: a randomized controlled trial. *Hum. Vaccin. Immunother.* 14, 1489–1500.
- van der Lubbe, J.E.M., Verspuij, J.W.A., Huizingh, J., Schmit-Tillemans, S.P.R., Tolboom, J., Dekking, L., Kwaks, T., Brandenburg, B., Meijberg, W., Zahn, R.C., et al. (2018). Mini-HA is superior to full length hemagglutinin immunization in inducing stem-specific antibodies and protection against group 1 influenza virus challenges in mice. *Front. Immunol.* 9, 2350.
- van Erp, E.A., Luytjes, W., Ferwerda, G., and van Kasteren, P.B. (2019). Fc-Mediated antibody effector functions during respiratory syncytial virus infection and disease. *Front. Immunol.* 10, 548.
- Wise, M.C., Xu, Z., Tello-Ruiz, E., Beck, C., Trautz, A., Patel, A., Elliott, S.T., Chokkalingam, N., Kim, S., Kerkau, M.G., et al. (2020). In vivo delivery of synthetic DNA-encoded antibodies induces broad HIV-1-neutralizing activity. *J. Clin. Invest.* 130, 827–837.
- Xu, Z., and Kulp, D.W. (2019). Protein engineering and particulate display of B-cell epitopes to facilitate development of novel vaccines. *Curr. Opin. Immunol.* 59, 49–56.
- Xu, Z., Wise, M.C., Choi, H., Perales-Puchalt, A., Patel, A., Tello-Ruiz, E., Chu, J.D., Muthumani, K., and Weiner, D.B. (2018). Synthetic DNA delivery

by electroporation promotes robust in vivo sulfation of broadly neutralizing anti-HIV immunoadhesin eCD4-Ig. *EBioMedicine* 35, 97–105.

Xu, Z., Wise, M.C., Chokkalingam, N., Walker, S., Tello-Ruiz, E., Elliott, S.T.C., Perales-Puchalt, A., Xiao, P., Zhu, X., Pumroy, R.A., et al. (2020). In vivo assembly of nanoparticles achieved through

synergy of structure-based protein engineering and synthetic DNA generates enhanced adaptive immunity. *Adv. Sci. (Weinh)* 7, 1902802.

Yassine, H.M., Boyington, J.C., McTamney, P.M., Wei, C.J., Kanekiyo, M., Kong, W.P., Gallagher, J.R., Wang, L., Zhang, Y., Joyce, M.G., et al. (2015). Hemagglutinin-stem nanoparticles

generate heterosubtypic influenza protection. *Nat. Med.* 21, 1065–1070.

Zhang, X., Ing, S., Fraser, A., Chen, M., Khan, O., Zakem, J., Davis, W., and Quinet, R. (2013). Follicular helper T cells: new insights into mechanisms of autoimmune diseases. *Ochsner J.* 13, 131–139.

iScience, Volume 23

## Supplemental Information

### **Incorporation of a Novel CD4+ Helper Epitope Identified from *Aquifex aeolicus* Enhances Humoral Responses Induced by DNA and Protein Vaccinations**

**Ziyang Xu, Neethu Chokkalingam, Edgar Tello-Ruiz, Susanne Walker, Daniel W. Kulp, and David B. Weiner**

## Supplemental Figures and Table

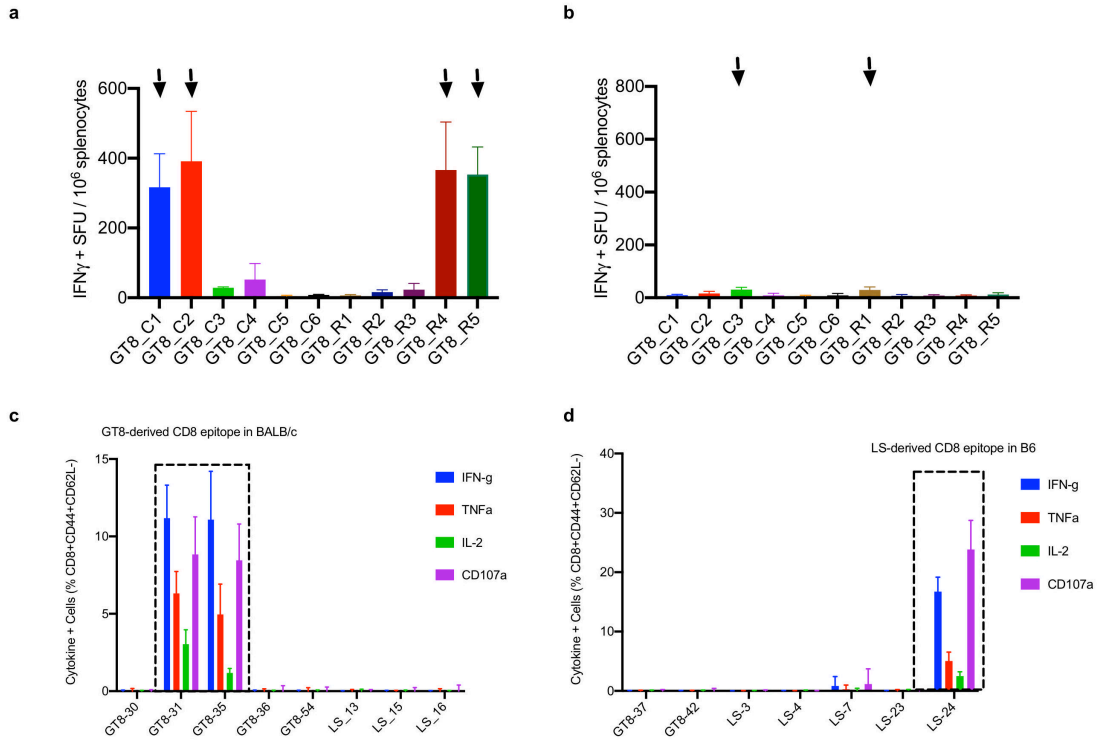


**Figure S1. CD8+ T-cell epitopes in DLnano\_LS\_GT8 were mapped to the GT8 and LS domains in BALB/c and C57BL/6 mice, respectively. Related to Figure 1.** Mice received 25ug DNA vaccination with EP twice three weeks apart and were euthanized two weeks post the second vaccination for cellular analysis. **a** and **b**. Matrix mapping by IFN $\gamma$  ELISpot assays in the GT8 domain to determine the dominant T-cell epitopes in BALB/c (**a**) or C57BL/6 (**b**) mice. **c**. and **d**. Identification of the dominant CD8+ T-cell epitope by ICS in the GT8 domain for BALB/c mice (**c**) and in the LS domain for C57BL/6 mice (**d**). Each group includes five mice; error bar represents standard deviation; arrow above the bar graph represents the dominant peptide pool identified.

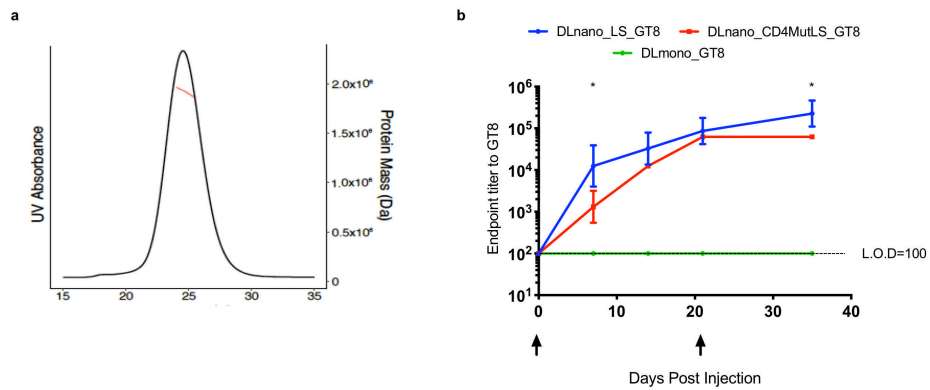


**Figure S2. Knock out of the LS-3 epitope from DLnano\_LS\_GT8 was observed to attenuate vaccine-induced humoral immunity. Related to Figure 3.** Mice were immunized in the same manner as described in **Figure 3a**. SEC-MAL trace of SEC-purified CD4MutLS\_GT8; the molecular weight was determined to be around 2MDa for CD4MutLS\_GT8. **b.** Humoral responses induced to GT8 by two doses of DLnano\_CD4MutLS\_GT8 in comparison to DLnano\_LS\_GT8 and DLmono\_GT8, as assessed by ELISA; p-values compare differences between DLnano\_CD4MutLS\_GT8 and DLnano\_LS\_GT8 at each timepoint. Each group includes five mice; error bar represents standard deviation; two-tailed Mann-Whitney Rank Test used to compare groups; \*, p-value<0.05.

a

Peptide	PADRE	LS3
Number of Residues	13	15
Molecular Weight g/mol	1348	1624
Iso-electric point (pH)	10.7	12.1
Net Charge at pH 7	2.0	2.1
Water solubility	Poor	Poor

b

Peptide: PADRE- AKFVAAWTLKAAA				
	allele	smm_align_ic50 (nM)	nn_align_ic50 (nM)	Measured_ic50 (nM)
Human	HLA-DRB1*07:01	144	17.9	1.2
	HLA-DRB5*01:01	179	11.8	18
	HLA-DRB3*01:01	1262	310.2	1470
Murine	H2-lab	677	95.8	44

c

Peptide	LS3	PADRE	FC_CH1 <sub>1-15</sub>
	LRFGIVASRANHALV	AKFVAAWTLKAAA	ASTKGPSVFPLAPSS
DRB1_01_01 *	0.369	3.66	89.5
DRB1_01_02 *	0.16	9.19	89.3
DRB1_01_03	0.409	0.504	90
DRB1_03_01 *	1.74	12	72
DRB1_04_01	1.16	0.046	15.8
DRB1_04_04 *	0.755	4.72	50.8
DRB1_04_05	6.41	1.97	27.9
DRB1_04_08	1.67	0.0995	16
DRB1_07_01 *	0.63	3.46	73.1
DRB1_08_01	6.53	9.02	90.3
DRB1_10_01	1.52	2.49	57.3
DRB1_11_01	3.75	0.0901	83.1
DRB1_11_04	1.5	1.27	74.2
DRB1_12_01	8.03	17.2	69.9
DRB1_13_01	1.81	2.16	69.4
DRB1_13_03	1.02	3.42	80.3
DRB1_15_01 *	3.12	10.5	31
DRB1_16_01 *	1.31	3.5	67.4
DRB3_01_01 *	2.99	11.6	62.3
DRB3_02_02 *	0.281	12.1	15.3
DRB4_01_01	4.62	12.4	12.5
DRB4_01_03	6.66	13.5	12.9
DRB5_01_01	4.31	10.2	90
DRB5_02_02 *	0.76	6.09	48.3
Geometric mean	1.59	3.08	48.10

**Figure S3. LS3 and PADRE epitopes were observed to have complementary coverage in binding to different human HLA-DR alleles. Related to Figure 4.** **a.** Comparison of predicted biophysical properties between PADRE and LS-3, in terms of molecular weight, isoelectric point, net charge at pH 7 and water solubility. **b.** Comparison of predicted IC50 binding affinities of PADRE epitope to human DRB1\_07\_01, DRB5\_01\_01, DRB3\_01\_01 and murine HLA-lab by smm-align and nn-align versus reported experimentally measured IC50 binding affinities (Alexander et al., 1994). **c.** Comparison of predicted IC50 binding affinities (in terms of percentile rank, 0-100) of LS-3, PADRE, and Fc-CH1<sub>1-15</sub> epitopes to various human HLA-DR alleles by MixMHCIIpred (Racle et al., 2019); a lower percentile rank is suggestive of higher binding affinity.

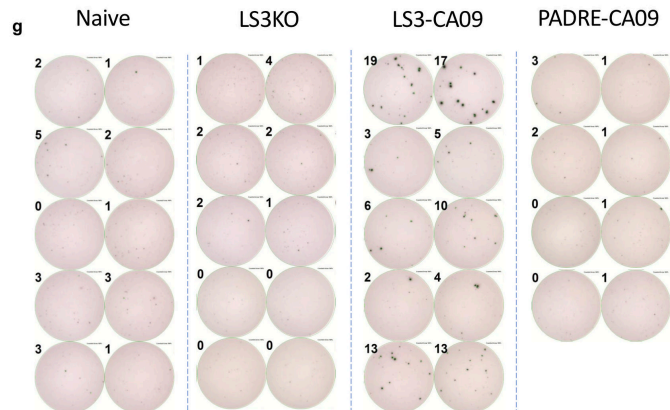
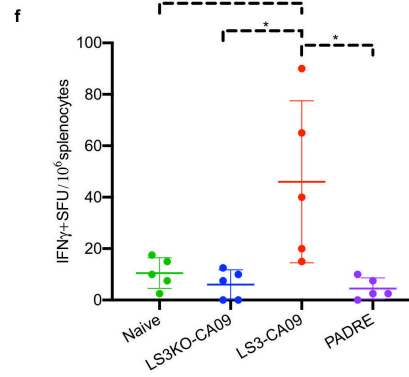
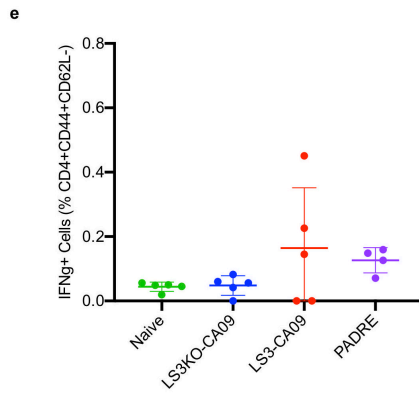
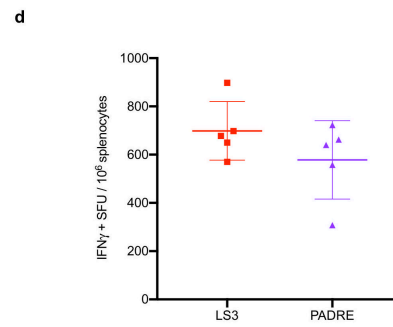
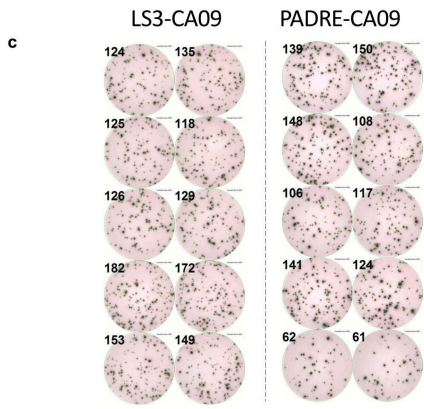
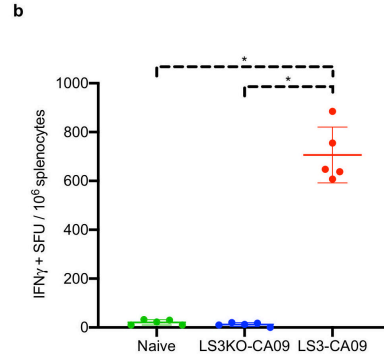
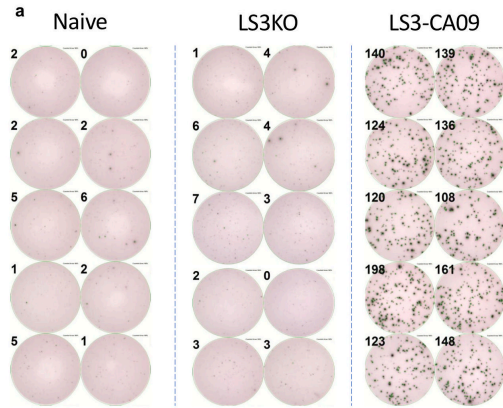


**Figure S4. The LS-3 and PADRE epitopes were observed to elicit epitope-specific CD4<sup>+</sup> T-cell responses by DNA vaccination, and to a lesser extent, by protein vaccination. Related to Figure 4.**

C57BL/6 mice received either DNA or protein vaccinations and were euthanized as described in Figure 4. **a** and **b**. IFN $\gamma$ <sup>+</sup> ELISpot assays comparing T-cell responses induced by either DNA-encoded LS3-CA09 or LS3KO-CA09 immunizations in mice to LS3 and LS3KO peptides respectively. **c** and **d**. IFN $\gamma$ <sup>+</sup> ELISpot assays comparing T-cell responses induced by either DNA-encoded LS3-CA09 or PADRE-CA09 immunizations in mice to LS3 and PADRE peptides respectively. **e**. ICS analysis of CD4<sup>+</sup> IFN $\gamma$ <sup>+</sup> responses induced by protein LS3KO-CA09, LS3-CA09, or PADRE-CA09 vaccinations in mice to LS3KO, LS3, and PADRE peptides respectively. **f** and **g**. IFN $\gamma$ <sup>+</sup> ELISpot assays comparing T-cell responses induced by protein LS3KO-CA09, LS3-CA09, or PADRE-CA09 vaccinations in mice to LS3KO, LS3, and PADRE peptides respectively. Each group includes five mice; each dot represents a mouse; error bar represents standard deviation; two-tailed Mann-Whitney Rank Test used to compare groups; p-values were adjusted for multiple comparison where appropriate; \*, p-value<0.05.

Strain	Category	Domain	Sequence	Classification
<b>BALB/c</b>	CD4	Lumazine Synthase	DAVIAIGVLCRGATP	WT
		Lumazine Synthase	ATPSFDYIASEVSKG	WT
	CD8	GT8	TRQGGYSNDNTVIFR	WT
		GT8	ARCQIAGTVVSTQLF	WT
<b>C57BL/6</b>	CD4	Lumazine Synthase	LRFGIVASRANHALV	WT
		Lumazine Synthase	LKFGIVGSRFNHGLV	LS3KO
	CD8	Lumazine Synthase	AALCAIEMANLFKSL	WT

**Table S1. Identified CD4+ and CD8+ epitopes in the LS and GT8 domains in the BALB/c and C57BL/6 mice immunized twice with 25ug DLnano\_LS\_GT8 three weeks apart and sacrificed two weeks post the second vaccination for cellular analysis. Related to Figure 1.**

## Transparent Methods

### *Structure modeling and design of CD4Mut\_LS\_GT8 nanoparticles*

Mutations to the LS-3 peptide were achieved using a structure-guided process. First, positions 14, 19, 22 and 24 in the LS domain were selected for mutation because they were making minimal contacts to the rest of the LS 1HQK crystal structure, which we hypothesized would have less detrimental effect on protein folding. Second, we used the 'fixbb' application of ROSETTA to computationally mutate the selected positions to each of the 20 amino acids allowing neighboring residues to change conformation. Mutations were selected which had similar or lower total score relative to the wild-type amino acid and by visual inspection of the resulting structural models. The mutations were R14K, A19G, A22F, A24G.

### *DNA design and plasmid synthesis*

Protein sequences for IgE Leader Sequence and eOD-GT8-60mer were as previously reported (Briney et al., 2016; Xu et al., 2018). DNA encoding protein sequences were codon and RNA optimized as previously described (Xu et al., 2018). The optimized transgenes were synthesized de novo (GenScript) and cloned into a modified pVAX-1 backbone under the control of the human CMV promoter and bovine growth hormone poly-adenylation signal.

### *Production of His-Tagged LS3-CA09, LS3KO-CA09, or PADRE-CA09*

Expi293F cells were transfected with pVAX plasmid vector carrying the His-Tagged LS3-CA09, LS3KO-CA09, PADRE-CA09, GT8-monomer, eOD-GT8-60mer or CD4Mut\_LS\_GT8-60mer transgene with PEI/OPTI-MEM and harvested 6 days post-transfection. Transfection supernatant was first purified with affinity chromatography using the AKTA pure 25 system and an IMAC Nickel column for His-Tagged constructs and gravity flow columns filled with GNL Lectin beads (for nanoparticles). The eluate fractions from the affinity purification were pooled, concentrated and dialyzed into 1X PBS buffer before being loaded onto the SEC column and then purified with size exclusion chromatography with the Superdex 200 10/300 GL column (GE Healthcare) for His-Tagged constructs, and with Superose 6 Increase 10/300 GL column for nanoparticles. Identified eluate fractions were then collected and concentrated to 1mg/mL in PBS.

### *Animals*

All animal experiments were carried out in accordance with animal protocols 201214 and 201115 approved by the Wistar Institute Institutional Animal Care and Use Committee (IACUC). For DNA-based immunization, 6 to 8 week old female C57BL/6 or BALB/c mice (Jackson Laboratory) were immunized with DNA vaccines via intramuscular injections into the tibialis anterior muscles, coupled with intramuscular EP with the CELLECTRA 3P device (Inovio Pharmaceuticals). In experiments in Figure 1 and 3, mice were immunized twice with 25ug DNA plasmid three weeks apart and euthanized two weeks post the second vaccination. In experiments in Figure 4, mice were immunized twice with 25ug DNA plasmid twice four weeks apart and

euthanized one week post the second vaccination. For vaccinations involving recombinant protein, 6 to 8-week-old female C57BL/6 mice were immunized intramuscularly with 10ug of recombinant LS3-CA09, LS3KO-CA09 or PADRE-CA09 protein in 15uL sterile PBS co-formulated with 15uL Sigma Adjuvant System (SigmaAldrich) in the tibialis anterior muscles three times four weeks apart and were euthanized one week post the third immunization.

#### *HA-binding ELISA*

96-well half area plates were coated at 4C overnight with 2ug/mL of recombinant HA( $\Delta$ TM)( A/California/04/2009) (Immune Technology), and blocked at room temperature for 2 hour with a solution containing 1x PBS, 5% skim milk, 10% goat serum, 1% BSA, 1% FBS, and 0.2% Tween-20. The plates were subsequently incubated with serially diluted mouse sera at 37C for 2 hours, followed by 1-hour incubation with anti-mouse IgG H+L HRP (Bethyl) at 1:20,000 dilution at room temperature and developed with TMB substrate. Absorbance at 450nm and 570nm were recorded with BioTEK plate reader.

#### *Antigenic profile characterization of purified eOD-GT8-60mer and CD4Mut\_LS\_GT8-60mer*

Corning half-area 96-well plates were coated with 2ug/mL of purified eOD-GT8-60mer or CD4Mut\_LS\_GT8-60mer at 4C overnight. The plates were then blocked with the buffer as described above for 2 hours at room temperature, followed by incubation with serially diluted VRC01 at room temperature for 2 hours. The plates were then incubated with anti-human Fc (cross-adsorbed against rabbits and mice) (Jackson Immunoresearch) at 1:10,000 dilution for 1 hour, followed by addition of TMB substrate for detection. Absorbance at 450nm and 570nm were recorded with BioTEK plate reader.

#### *HAI assay*

Mice sera were treated with receptor-destroying enzyme (RDE, 1:3 ratio; SEIKEN) at 37°C overnight for 18–20 h followed by complement and enzyme inactivation at 56°C for 45 min. RDE-treated sera were subsequently cross-adsorbed with 10% rooster red blood cells (Lampire Biologicals) in 0.9% saline at 4C for 1 hour. The cross-adsorbed sera were then serially diluted with PBS in a 96-well V-bottom microtiter plates (Corning). Four hemagglutinating doses (HAD) of A/California/07/2009 (H1N1)pdm09 (Virapur) were added to each well and the serum–virus mixture was incubated at room temperature for 1 hour. The mixture was then incubated with 50  $\mu$ l 0.5% v/v rooster red blood cells in 0.9% saline for 30 min at room temperature. The HAI antibody titer was scored with the dot method, and the reciprocal of the highest dilution that did not cause agglutination of the rooster red blood cells was recorded.

#### *ELISpot Assay*

Spleens from immunized mice were collected and homogenized into single cell suspension with a tissue stomacher in 10% FBS/ 1% Penicillin- streptomycin in RPMI 1640. Red blood cells were subsequently lysed with ACK lysing buffer (ThermoFisher) and percentage of viable cells were determined with Trypan Blue

exclusion using Vi-CELL XR (Beckman Coulter). 200,000 cells were then plated in each well in the mouse IFN $\gamma$  ELISpot plates (MabTech), followed by addition of peptide pools that span both the lumazine synthase, 3BVE, PfV or GT8 domains, or individual LS-3, LS3KO or PADRE peptides at 5 $\mu$ g/mL of final concentration for each peptide (GenScript). The cells were then stimulated at 37C for 16-18 hours, followed by development according to the manufacturer's instructions. Spots for each well were then imaged and counted with ImmunoSpot Macro Analyzer.

#### *Intracellular cytokine staining*

Single cell suspension from spleens of immunized animals were prepared as described before and stimulated with 5 $\mu$ g/mL of peptides (GenScript) for 5 hours at 37C in the presence of 1:500 protein transport inhibitor (ThermoFisher). The cells were then incubated with live/dead for 10 min at room temperature, surface stains (anti-mouse CD4 BV510, anti-mouse CD8 APC-Cy7, anti-mouse CD44 AF700, anti-mouse CD62L BV771) (BD-Biosciences) at room temperature for 30minutes. The cells were then fixed and permeabilized according to manufacturer's instructions for BD Cytoperm Cytofix kit and stained with intracellular stains anti-mouse IL-2 PE-Cy7, anti-mouse IFN- $\gamma$  APC, anti-mouse CD3e PE-Cy5 and anti-mouse TNF $\alpha$  BV605 (BioLegend) at 4C for 1 hour. The cells were subsequently analyzed with LSR II 18-color flow cytometer.

#### *Epitope mapping*

15-mer peptides spanning the LS and GT8 domains of eOD-GT8-60mer (GenScript) were arranged into row and column pools (each peptide appears exactly once in the row pool and once in the column pool). Splenocytes from BALB/c or C57BL/6 immunized twice with 25 $\mu$ g DLnano\_LS\_GT8 were co-incubated with each peptide pool with a final concentration of 5 $\mu$ g/mL for each peptide overnight in IFN $\gamma$  ELISpot plates (MabTech). The plates were then developed according to manufacturer's instruction, and peptides that can potentially stimulate T-cell responses were identified based on the combination of row and column pools that induce IFN $\gamma$  responses. Responses to those peptides were then confirmed with ICS as described in the last section.

#### *In silico analysis*

Binding analysis prediction using smm- and nn-align was performed with a web-based application at the following site (<http://tools.iedb.org/mhcii/>) (Nielsen and Lund, 2009; Nielsen et al., 2007). Binding analysis prediction using the MixMHCIIpred model was executed with C++ using the codes available at the following site (<http://mixmhc2pred.gfellerlab.org/>) (Racle et al., 2019).

#### *Statistics*

Power analysis was performed with R based on our preliminary data to determine the smallest sample size that would allow us to achieve a power of 0.9 with a pre-set  $\alpha$ -value of 0.05. All statistical analyses were

performed with PRISM V8.2.1 and R V3.5.1. Each individual data point was sampled independently. Two-tailed Mann Whitney Rank Tests were used to compare differences between groups. Bonferroni corrections were used to adjust for multiple comparisons.

## Supplemental References

- Alexander, J., Sidney, J., Southwood, S., Ruppert, J., Oseroff, C., Maewal, A., Snoke, K., Serra, H.M., Kubo, R.T., Sette, A., *et al.* (1994). Development of high potency universal DR-restricted helper epitopes by modification of high affinity DR-blocking peptides. *Immunity* *1*, 751-761.
- Briney, B., Sok, D., Jardine, J.G., Kulp, D.W., Skog, P., Menis, S., Jacak, R., Kalyuzhniy, O., de Val, N., Sesterhenn, F., *et al.* (2016). Tailored Immunogens Direct Affinity Maturation toward HIV Neutralizing Antibodies. *Cell* *166*, 1459-1470 e1411.
- Nielsen, M., and Lund, O. (2009). NN-align. An artificial neural network-based alignment algorithm for MHC class II peptide binding prediction. *BMC Bioinformatics* *10*, 296.
- Nielsen, M., Lundegaard, C., and Lund, O. (2007). Prediction of MHC class II binding affinity using SMM-align, a novel stabilization matrix alignment method. *BMC Bioinformatics* *8*, 238.
- Racle, J., Michaux, J., Rockinger, G.A., Arnaud, M., Bobisse, S., Chong, C., Guillaume, P., Coukos, G., Harari, A., Jandus, C., *et al.* (2019). Robust prediction of HLA class II epitopes by deep motif deconvolution of immunopeptidomes. *Nat Biotechnol* *37*, 1283-1286.
- Xu, Z., Wise, M.C., Choi, H., Perales-Puchalt, A., Patel, A., Tello-Ruiz, E., Chu, J.D., Muthumani, K., and Weiner, D.B. (2018). Synthetic DNA delivery by electroporation promotes robust in vivo sulfation of broadly neutralizing anti-HIV immunoadhesin eCD4-Ig. *EBioMedicine* *35*, 97-105.